The Effect of Climate Change on the Variability of the Northern Hemisphere Stratospheric Polar Vortex

DANIEL M. MITCHELL, SCOTT M. OSPREY, AND LESLEY J. GRAY

National Centre for Atmospheric Science, University of Oxford, Oxford, United Kingdom

NEAL BUTCHART AND STEVEN C. HARDIMAN

Met Office Hadley Centre, Exeter, United Kingdom

ANDREW J. CHARLTON-PEREZ

Department of Meteorology, Reading University, Reading, United Kingdom

PETER WATSON

Atmospheric, Oceanic and Planetary Physics, University of Oxford, Oxford, United Kingdom

(Manuscript received 13 January 2012, in final form 12 March 2012)

ABSTRACT

With extreme variability of the Arctic polar vortex being a key link for stratosphere–troposphere influences, its evolution into the twenty-first century is important for projections of changing surface climate in response to greenhouse gases. Variability of the stratospheric vortex is examined using a state-of-the-art climate model and a suite of specifically developed vortex diagnostics. The model has a fully coupled ocean and a fully resolved stratosphere. Analysis of the standard stratospheric zonal mean wind diagnostic shows no significant increase over the twenty-first century in the number of major sudden stratospheric warmings (SSWs) from its historical value of 0.7 events per decade, although the monthly distribution of SSWs does vary, with events becoming more evenly dispersed throughout the winter. However, further analyses using geometric-based vortex diagnostics show that the vortex mean state becomes weaker, and the vortex centroid is climatologically more equatorward by up to 2.5°, especially during early winter. The results using these diagnostics not only characterize the vortex structure and evolution but also emphasize the need for vortex-centric diagnostics over zonally averaged measures. Finally, vortex variability is subdivided into wave-1 (displaced) and -2 (split) components, and it is implied that vortex displacement events increase in frequency under climate change, whereas little change is observed in splitting events.

1. Introduction

It is well documented that under increased greenhouse gas (GHG) emissions a globally averaged tropospheric warming and stratospheric cooling is expected. The stratospheric cooling can be attributed to decreased amounts of outgoing infrared radiation reaching the stratospheric CO_2 molecules (Fels et al. 1980; Clough and Iacono 1995; Bell et al. 2010). Adding to the complexity of the situation are the expected changes in future stratospheric concentrations of ozone-depleting substances and the subsequent temperature changes that result from ozone recovery (e.g., Son et al. 2008). The interaction between the stratospheric response to GHGs and ozone changes results in a complex nonlinear dynamical response (e.g., Waugh et al. 2009), and it has been shown previously that one of the key dynamical features in the stratosphere for influencing surface climate is the Northern Hemisphere (NH) polar vortex (Baldwin and Dunkerton 2001; Mitchell et al. 2012a, manuscript submitted to *J. Climate*).

The polar vortex is evident as a region of strong westerly winds in the NH winter at high latitudes. During

Corresponding author address: Daniel Mitchell, Atmospheric, Oceanic and Planetary Physics, University of Oxford, Oxford OX1 3PU, United Kingdom.
E-mail: mitchell@atm.ox.ac.uk

DOI: 10.1175/JAS-D-12-021.1

the vortex ''final warming'' the westerlies reverse as the hemisphere transitions radiatively into its summer regime of easterlies. However, the vortex can also be broken down purely by dynamics during midwinter in an event known as a major sudden stratospheric warming (SSW). These events are associated with increased levels of vertically propagating Rossby waves that are able to travel through regions of westerly winds by virtue of the Charney–Drazin criterion (Charney et al. 1961). Such large-scale dynamical events have been linked with tropospheric blocking (Woollings et al. 2010) and have been shown to influence surface climate directly (e.g., Baldwin and Dunkerton 2001; Thompson et al. 2002; Mitchell et al. 2012a, manuscript submitted to *J. Climate*) and indirectly through changes in ozone chemistry (e.g., Schoeberl and Hartmann 1991). SSW events have been classified in many different ways; for instance, Charlton and Polvani (2007) define an SSW as when ''the zonal mean zonal wind at 60°N and 10 hPa reverses from westerly to easterly.'' Other studies have used definitions based on the leading patterns in various dynamical fields, termed ''annular modes'' (e.g., Baldwin and Thompson 2009). Yet more studies have considered geometric definitions of the vortex, collectively known as ''moment diagnostics'' or ''elliptical diagnostics,'' that measure the location, shape, and size of the vortex (Waugh 1997; Waugh and Randel 1999; Matthewman et al. 2009; Mitchell et al. 2011a,b).

The use of these varying diagnostics, as well as differing complexities in models used to study these extreme events, have led to no clear consensus on whether vortex disturbances will increase into the future (e.g., Charlton-Perez et al. 2008) or decrease (e.g., Rind et al. 1998). For instance, Bell et al. (2010) found that under 4 times preindustrial CO_2 conditions the frequency of SSWs was doubled compared with its control state. They also noted that at 2 times preindustrial CO_2 conditions no statistically significant increase in SSWs was observed, and that these conditions were more comparable to the projected climate scenarios described in the assessments of the Intergovernmental Panel on Climate Change (IPCC). Likewise, Charlton-Perez et al. (2008) showed using the Atmospheric Model with Transport and Chemistry (AMTRAC) and a middle-of-the-road anthropogenic forcing scenario that SSWs would increase by 1 event per decade by the end of the twenty-first century. McLandress and Shepherd (2009) also observed an increase in SSWs into the future using the zonal wind–based definitions, although they suggest that this is due to a decrease in the climatology of the winds, allowing the standard SSW criterion to be more easily met. Hence they argue that using a relative definition such as the northern annular mode (NAM) is more appropriate, and in doing so they find no change in SSWs.

Some of the discrepancies between these studies may well be due to models including or excluding coupled chemistry modules, or coupled oceans, as well insufficient vertical and horizontal resolutions in the stratosphere. For instance, the fine filamentations of vortex air that are continuously mixed into the background flow would be hard to capture with a coarse resolution. Mitchell et al. (2011a) showed that a horizontal resolution of $5° \times 5°$ was at the extreme end of what was acceptable. Additional discrepancies may also be due to how well individual models characterize competing effects from 1) the radiative state in the stratosphere, leading to vortex strengthening by infrared radiative cooling, and 2) Rossby wave sources in the troposphere, leading to enhanced upward wave propagation and to vortex weakening.

Because of the aforementioned arguments it is often insightful to use multimodel ensembles in order to reduce model uncertainties. Butchart et al. (2011) show that the multimodel mean of 16 coupled chemistry–climate models (CCMs) predict that Rossby wave activity entering the stratosphere will not change dramatically over the twenty-first century. Mitchell et al. (2012b) strengthened this conclusion by showing with an ensemble of CCMs that the frequency of extreme vortex variability in terms of the location and geometry of the vortex did not seem to change notably over the twenty-first century under a more realistic climate scenario forcing.

The aforementioned studies have thus demonstrated a range in predictions of vortex variability under a change in radiative forcing scenarios. In this study we extend these investigations using a state-of-the-art climate model that has both a fully resolved stratosphere and a fully coupled ocean. In this way the importance of coupled ocean feedbacks in, for example, generating ocean–land contrasts and Rossby wave trains into the stratosphere is included. Two principal techniques are employed to compare and contrast vortex variability. The standard zonally averaged zonal wind diagnostics (Charlton and Polvani 2007) and the moment-based diagnostics (Mitchell et al. 2011a). Whereas the zonal wind definition is more commonly used and is easily interpreted, the moment-based definition is based on potential vorticity (PV) distributions and does not rely on a threshold criterion. It therefore provides a relative criterion to test future vortex variability and avoids the problems arising from a change in background state identified by McLandress and Shepherd (2009). A more technical discussion of these diagnostics is given in section 3.

2. Experimental details

We use version 2 of the Hadley Centre global environmental model with a coupled carbon cycle (HadGEM2-CC), described in detail by Martin et al. (2011) and Jones et al. (2011). This particular configuration of the model has 40 vertical levels in the ocean, coupled with 60 vertical levels in the atmosphere and a lid at 84 km. The model does not include coupled chemistry; monthly averaged distributions of ozone and greenhouse gases are imposed in the radiation scheme. Realistic variations of radiative forcing are imposed, including greenhouse gases, ozone, aerosols, and solar and volcanic forcing. The historical simulations are run from 1860 to 2005 and are as specified for phase 5 of the Coupled Model Intercomparison Project (CMIP5). The model has also been run into the future, following the RCP8.5[1] scenario out to the year 2100. A more complete overview of the historical stratospheric climatology, variability, and its influence on surface climate is given in Hardiman et al. (2012).

Three ensemble members are employed in this study, two of which run from 1960 to 2100 and one from 1860 to 2100. Over the course of this study all ensemble members are used unless otherwise stated. A 240-yr control simulation is also used in which the model is run using preindustrial conditions with no varying radiative forcings, so that the internal variability may be estimated.

One noteworthy point is that HadGEM2-CC does not include interactive ozone chemistry because of limitations in computation time. A disadvantage of this is that CCMs tend to reproduce a better stratospheric mean state and variability than non-CCMs, as well as better tropospheric interannual variability (Butchart et al. 2011). As such, and considering that this study deals exclusively with the Arctic vortex, section 4a addresses these concerns.

3. Diagnostics

Throughout this study the standard SSW definitions using zonal mean zonal wind (ZMZW) and North Pole temperature are contrasted with the moment diagnostics that detail the vortex area, latitude of the centroid, and aspect ratio. A thorough description of these diagnostics is detailed in Mitchell et al. (2011a), and a brief description is given here for convenience. The moment diagnostics are defined by a standard 2D-moment equation, which in its natural form (i.e., in a frame of reference centered over the pole) is

$$\mu_{mn} = \sum_x \sum_y x^m y^n \hat{q}(x,y) \quad \text{for} \quad m + n \in \{0,1\} \quad (1)$$

and in its relative form (i.e., in a frame of reference centered over the polar vortex) is

$$\mu_{mn} = \sum_x \sum_y (x - \overline{x})^m (y - \overline{y})^n \hat{q}(x,y) \quad \text{for} \quad m + n \in \{2,\infty\}, \quad (2)$$

where m and n are the order of the moment in the x and y directions, respectively; $\overline{x}$ and $\overline{y}$ are the centroids of the vortex in the x and y directions, respectively; and $\hat{q}(x,y)$ is some conserved quantity on a particular 2D surface. Here, we set $\hat{q}(x,y)$ equal to PV in the Northern Hemisphere vortex region on isentropic surfaces as it is conserved under adiabatic and frictionless flow, as well as capturing the dynamical features of the polar vortex well (Waugh and Randel 1999). An objective measure of the vortex area is obtained by setting m and n equal to zero in Eq. (1) (i.e., $A_{\text{obj}} = \hat{q}A$, giving a measure of the vortex area A and strength). Note that the measure of vortex strength can be inferred as A_{obj} differs only from a circulation calculation in that PV is used in place of vorticity; hence, the two are different only by a factor of isentropic density [for more examples of this diagnostic, see Mitchell et al. (2011a,b)]. The vortex centroid latitude $(\overline{x}, \overline{y})$ is obtained from setting $m = 0, n = 1$ and $m = 1, n = 0$ in Eq. (1) and allows Eq. (2) to be used in calculating the higher-order moments. Finally, the vortex aspect ratio, defined as the major axis of the vortex divided by the minor axis, can be calculated from Eq. (2) by setting $m + n = 2$ [for more technical details, see Matthewman et al. (2009)].

4. Results

a. Zonal-mean diagnostics

To assess the reliability of HadGEM2-CC in simulating a realistic stratosphere, we begin the analysis by studying climatologies of the winter [December–February (DJF) average] zonal temperature and wind fields from the model compared with the 40-yr European Centre for Medium-Range Forecasts (ECMWF) Re-Analysis (ERA-40) (Fig. 1). The first two columns show respectively the climatologies in ERA-40 and the 240-yr control run, which has nonvarying, preindustrial GHG forcing. The third column shows the difference in climatologies in the transient run between 40 winters at the end of the historical period (1960–2000) and 40 winters at the end of the twenty-first century (2060–2100), which gives a measure of the atmospheric response to an increase in GHG. We note that by the end

[1] This scenario follows an increase in radiative forcing throughout the twenty-first century, which reaches a maximum of 8.5 W m^{-2} in 2100.

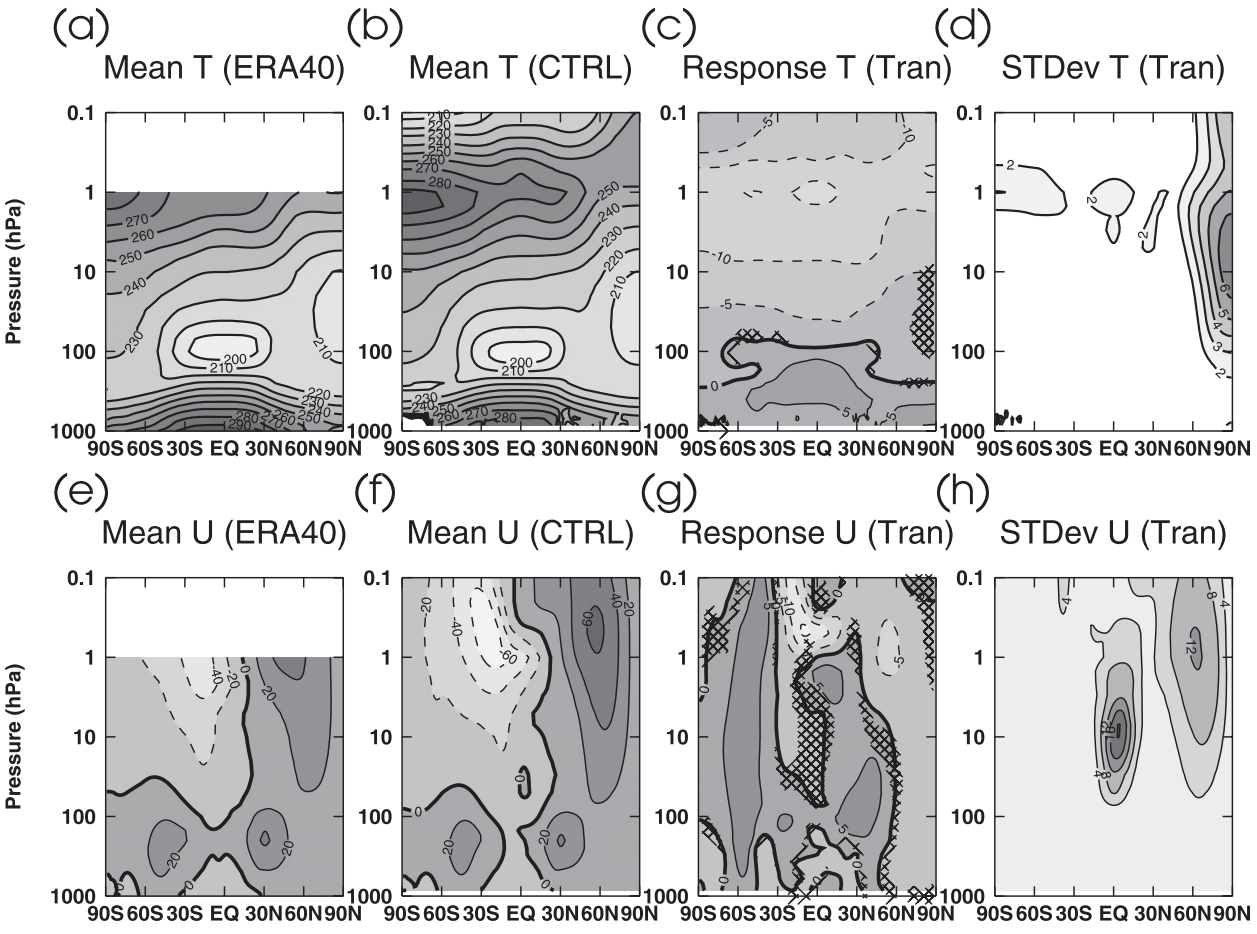

FIG. 1. DJF-averaged (top) zonal temperature and (bottom) zonal wind plots for (a),(e) the climatology in ERA-40, (b),(f) the climatology in the control, (c),(g) the difference between the 1960–2000 and 2060–2100 climatologies for the ensemble mean of the transient runs, and (d),(h) the standard deviation of the ensemble mean for the 1960–2000 period. Stippled areas indicate regions where the signal is not statistically significant at the 95% level using a *t* test.

of the twenty-first century the imposed ozone levels have recovered to pre–ozone hole levels and the differences in the stratospheric response by this time can be primarily attributed to increased GHG levels. The final column gives the standard deviation over the historical period as a measure of variability.

Figures 1a and 1b show the well-known temperature inversion associated with the stratosphere, with the northern polar stratosphere having cooler temperatures than elsewhere at similar heights (i.e., due to northern winter). The corresponding zonal winds (Figs. 1e,f) show the northern winter westerlies and the southern summer easterlies, and both the temperature and winds are in excellent agreement between the model and reanalysis. Figure 1c, which gives an indication of the change in the stratospheric temperature over the twenty-first century, shows stratospheric cooling and tropospheric heating due to increased GHG forcings. The maximum cooling is situated at the level of the stratopause, where the stratospheric temperatures are highest and therefore the longwave cooling to space associated with increased GHG levels is greatest. Above 1 hPa in the high southern latitudes the cooling is less than in the NH. This is likely to be due to a change in the mesospheric circulation associated with altered filtering of small-scale gravity waves by the changing background winds at lower levels. The corresponding plot for the zonal winds (Fig. 1g) shows a strengthening of the southern annular mode (SAM), which is in good agreement with Son et al. (2008, 2010) and a deceleration of the NH vortex winds, suggesting a more disturbed vortex. This result is similar to that found in Bell et al. (2010), who performed a 2 times preindustrial CO_2 equilibrium run using an earlier version of the Hadley Centre GCM. The RCP8.5 scenario employed in the current study corresponds to 3.3 times preindustrial CO_2 by the end of the twenty-first century, although this is a transient increase rather than the

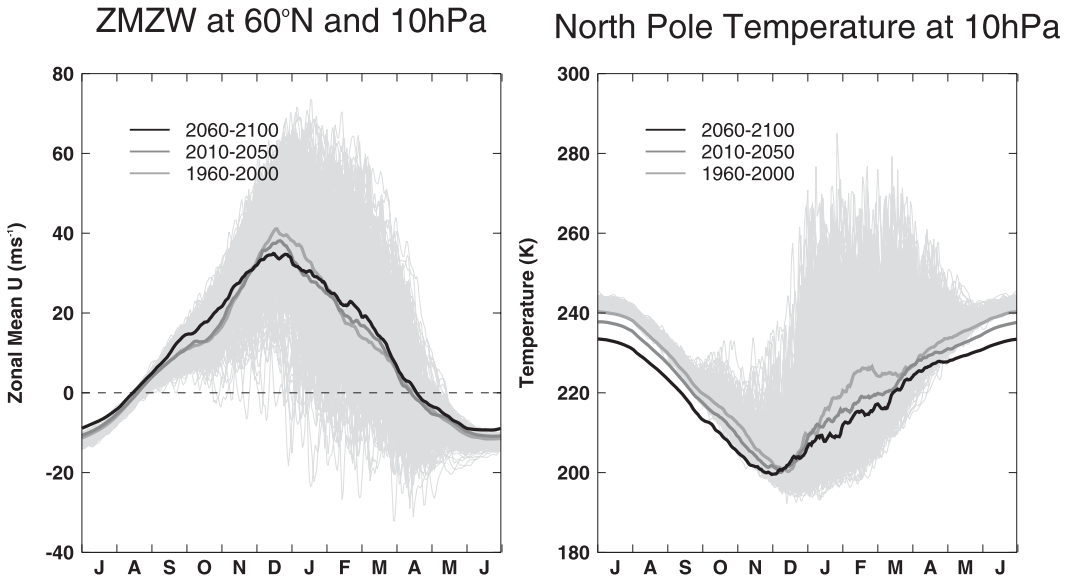

FIG. 2. Climatology of (left) zonal mean zonal wind at 60°N and 10 hPa and (right) North Pole temperature at 10 hPa for 1960–2000 (medium gray), 2010–2050 (dark gray), and 2060–2100 (black). In all cases the climatology is calculated from the ensemble mean of the transient runs. The annual time series for the preindustrial control data are plotted in light gray, to give a measure of the variance. The zero-wind line is dashed.

equilibrium case described by Bell et al. (2010). To understand better why certain areas are not significant, the third column in Fig. 1 gives a measure of variability in the fields. Figure 1h especially shows high levels of variability in the polar northern latitudes and also the equatorial region, and this is due to the presence of SSWs and the quasi-biennial oscillation (QBO), respectively, making it hard to achieve statistical significance. Indeed, Bell et al. (2010) found that it was not until the unrealistic scenario of 4 times preindustrial CO_2 was used that results became significant at these latitudes.

Focusing specifically on the vortex region, Fig. 2 shows the climatologies of (left) the ZMZW at 60°N and 10 hPa and (right) the temperature at the North Pole (90°N) and 10 hPa. The thick lines show progressively later periods in the analysis as progressively darker colors (the year-by-year data for the control run are also plotted with thin light gray lines underneath). The analysis for the zonal wind (left panel) shows no change in the final warming (i.e., the westerly–easterly wind transition during April) and little change in the mean state over the three periods.

The climatology of the North Pole temperature (right panel) changes in magnitude somewhat more than that of the ZMZW with a year-round cooling trend associated with increased outgoing infrared radiation to space. Examination of Figs. 1a and 1b shows cooling at the NH polar latitudes and yet an easterly wind anomaly, which suggests a more disturbed vortex. This appears to be contradictory, since a colder vortex usually implies a more stable vortex. However, it is actually the equator–pole temperature gradient that determines the zonal wind response and we note that equatorial temperatures are cooling at a faster rate than the polar temperatures, so the equator-to-pole temperature gradient is decreasing with time.

b. Stratospheric sudden warming frequency

Interestingly, in Fig. 2 no trend is observed in the average NP temperature during December but a large change is observed during February. This is due in part to the stratospheric temperature response during this period being largely influenced not only by radiative processes, but also by dynamical processes. To understand the dynamics better, we study SSW events and how they evolve over the twenty-first century.

Following the methodology of Charlton and Polvani (2007), we identify an SSW using the criteria of ZMZW reversal at 60°N and 10 hPa. This definition results in an SSW frequency of 0.70 events per winter for the 1960–2000 ensemble mean of the transient simulations, a greater value than about 0.6 events per winter obtained using ERA-40 and National Centers for Environmental Prediction (NCEP) reanalysis data over a similar period. This value increases to 0.78 events per winter in the latter half of the twenty-first century, suggesting a future increase in SSWs under this climate scenario. However, this result is not statistically significant within sampling errors, where the sampling error e can be determined

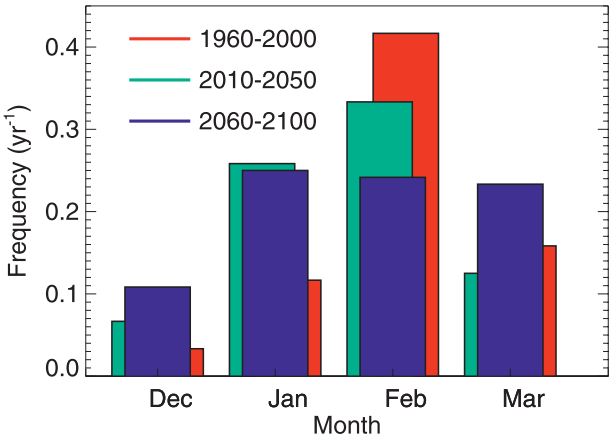

FIG. 3. The monthly distribution of SSW events for 1960–2000 (red), 2010–50 (green), and 2060–2100 (blue). SSWs are calculated using the method of Charlton and Polvani (2007).

from the sample variance s and the number of SSWs in each dataset N:

$$e = \left(\frac{s^2}{N}\right)^{1/2}. \quad (3)$$

However, Charlton et al. (2007) and Mitchell et al. (2012b) noted that monthly averaged analyses are more effective than winter-averaged analyses at diagnosing extreme vortex variability. Figure 3 therefore shows the month-by-month distribution of SSW events for the 1960–2000 (red), 2010–50 (green), and 2060–2100 periods (blue).

First, we note that the distribution of SSW events in the historical period (red) underestimates the number of early winter warmings when compared with ERA-40 (Charlton and Polvani 2007) and midwinter warmings tend to occur later than ERA-40 observations with the majority in February (Osprey et al. 2012, manuscript submitted to *J. Climate*). Charlton et al. (2007) note that late winter warmings is a common problem in models and suggest that this may be caused by early final warmings, although that does not seem to be the case in our model where final warmings occur, on average, during mid-April.

The distribution of SSWs does, however, become less peaked around February over the twenty-first century, and broader in nature, consistent in all three ensemble members (not shown). Interestingly, the distribution of SSWs in the 2060–2100 period (blue) is more like that of ERA-40 (over the 1960–2000 period).[2] The large decrease in SSWs during February may well be due to the increase in events during January, since an SSW is commonly followed by a cold period when Rossby waves are blocked by easterly winds at lower levels and the vortex is reestablished via radiative cooling. An equivalent analysis of the Southern Hemisphere vortex shows no major SSWs at any time in the past or future; while these events are rare in the reanalysis record, one such event did occur in 2002 but is still poorly understood (Charlton et al. 2005; Esler et al. 2006).

At this point it should be reiterated that our model simulations include stratospheric ozone depletion and recovery. In the historical period (1960–2000) ozone depletion occurs, peaking around 2000. As such less UV radiation is absorbed and hence causes a colder vortex. Conversely, in the latter half of the twenty-first-century ozone has mostly recovered and is at preindustrial levels; therefore the vortex would be warmer than otherwise. While the zero change in SSW frequency still holds for this study, it may well be due to competing effects between greenhouse gases and ozone changes.

As an expansion on this study Fig. 4 shows the frequency of SSWs in events per decade. The preindustrial control simulation has a frequency of between two and nine SSWs per decade, with a median value of five SSWs per decade, and this value is consistently exceeded by the ensemble mean of the transient simulations. The frequency of SSWs in the three transient ensemble members separately are also consistently larger than the control with maximum values ranging between 10 and 15 SSWs per decade over the twenty-first century, although the variability between ensemble members is large. The extreme value observed in 1980s of the second ensemble, which shows 15 events per decade, is due to many SSWs near the final warming date. This emphasizes the problems in dealing with an absolute valued definition (Mitchell et al. 2011a; Andrews et al. 1987) and highlights the problem discussed by McLandress and Shepherd (2009), who suggest that the zonal wind diagnostics can be misleading as a change in its climatology can effect a change in the number of events observed. Mitchell et al. (2012b) note that it is the presence of extreme variability of the polar vortex that is important for surface climate impacts, and not the absolute sign of the stratospheric winds, thus arguing for a direct estimate of vortex variability rather than a simple threshold estimate of whether the winds have changed to easterlies or not.

c. *Vortex-centric diagnostics*

While the analysis thus far yields an interesting insight into extreme vortex events, by the very binary nature of how the SSWs are defined, not all vortex variability can be captured. Mitchell et al. (2011a,b) demonstrated that use of the moment diagnostics (defined in section 3)

[2] As an aside, little is known at present about how the surface influence from SSWs varies as a function of occurrence within winter. While this analysis is beyond the scope of this study, it should be addressed in the near future.

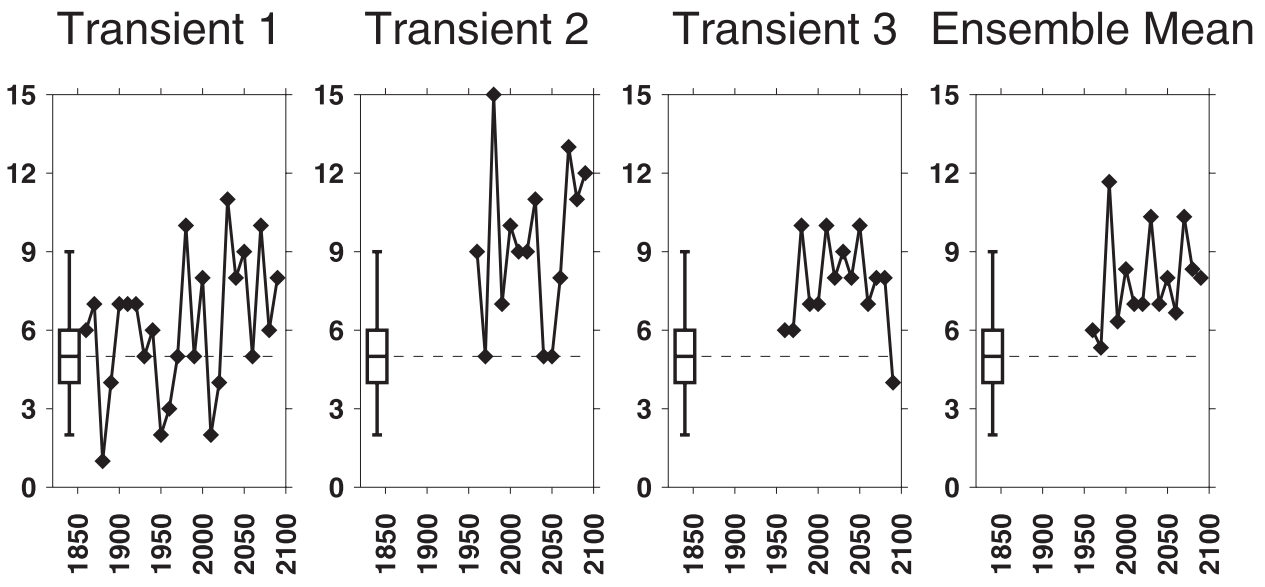

FIG. 4. The frequency of SSWs per decade for the three ensemble members of the transient runs as well as the ensemble mean. The range, interquartile range, and median of SSW frequency in the control run are also plotted as a box-and-whisker plot. The dashed line gives the median of SSWs per decade for the control.

greatly improved the analysis of vortex variability. We therefore use this to further understand the structure and evolution of the vortex over the twenty-first century.

As validation, Fig. 5 shows climatologies of each diagnostic compared with ERA-40 for the period 1960–2000 on the 840-K isentropic surface (~10 hPa). Most notable is the consistently weak vortex objective area (Fig. 5a). Recalling that this diagnostic is both a product of PV and vortex area and essentially gives a measure of the vortex strength (Matthewman et al. 2009), a further analysis reveals that this is due to the vortex PV being too weak in HadGEM2-CC compared with ERA-40. A similar conclusion was found in Mitchell et al. (2012b), who used a stratosphere-resolving coupled chemistry version of the same model but with no coupled ocean. The particularly low area during the late

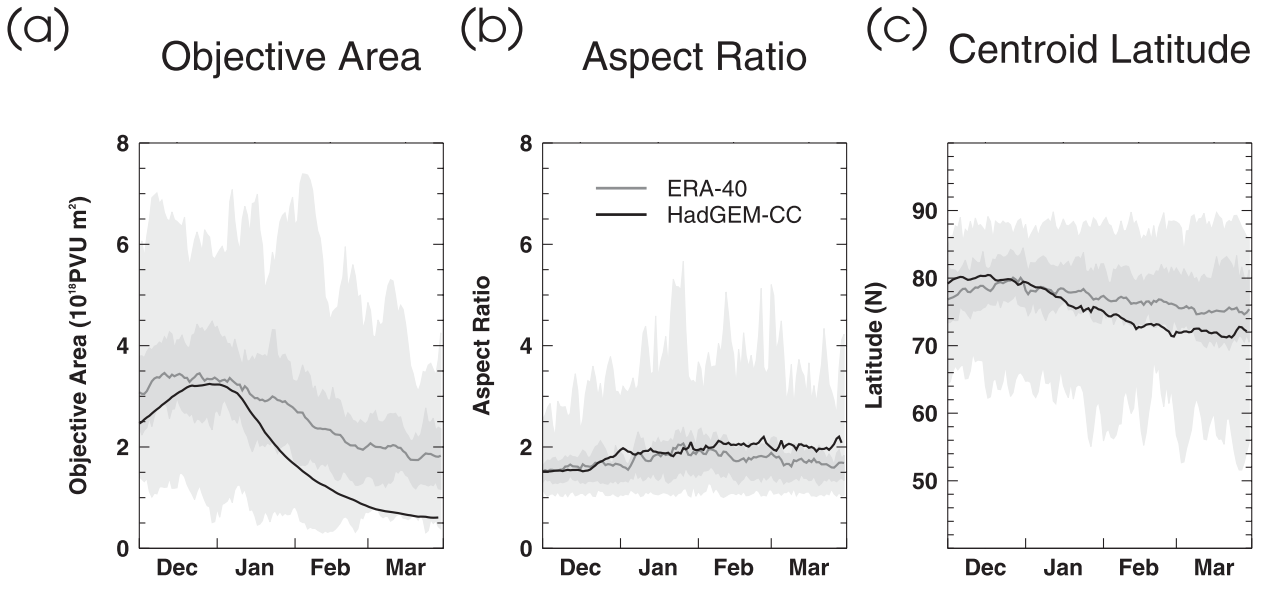

FIG. 5. Climatologies of the (a) vortex objective area, (b) centroid latitude, and (c) aspect ratio on the 840-K isentropic surface for the ensemble mean of the transient runs over 1960–2000 (black line) and ERA-40 over the same period (gray line). The range and interquartile range in ERA-40 are also plotted in light and medium gray, respectively.

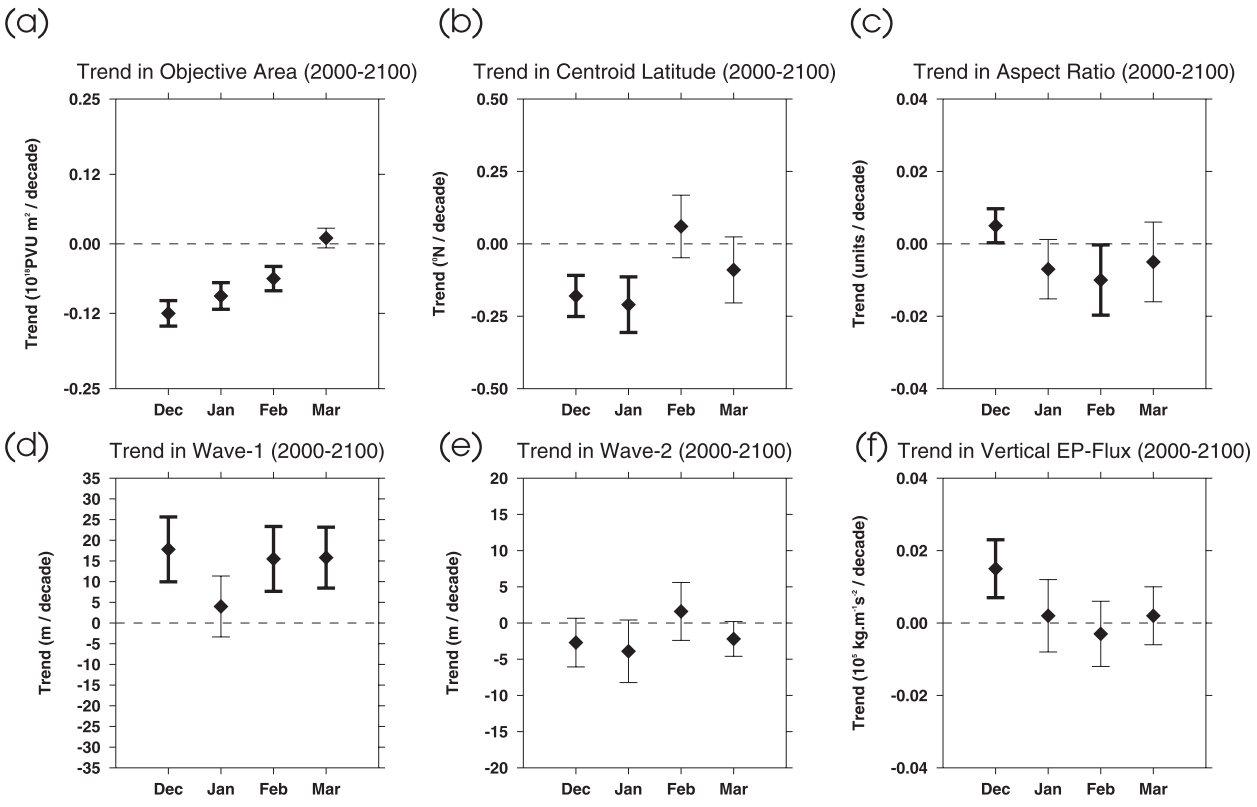

FIG. 6. Future (2000–2100) trends for the ensemble mean of the transient runs for (a) vortex objective area on the 840-K surface, (b) vortex centroid latitude on the 840-K surface, (c) vortex aspect ratio on the 840-K surface, (d) the amplitude of the wave-1 component of geopotential height at 10 hPa, (e) the amplitude of the wave-2 component of geopotential height at 10 hPa, and (f) the vertical component of EP flux measured at 100 hPa and 55°N. Whiskers represent 95% confidence intervals, and trends that are statistically significant from zero at the 95% level are thick.

winter is also consistent with Fig. 3, which shows too many late-winter SSWs, thereby weakening the vortex climatologically during this period.

The centroid-latitude climatology (Fig. 5c) is more equatorward in HadGEM2-CC in late winter than ERA-40, and this again suggests that the vortex is more disturbed than it should be during this period. The aspect ratio (Fig. 5b), however, shows no great deviation from that of ERA-40.

To determine how these diagnostics vary over the twenty-first century, Fig. 6 shows trends in the monthly averaged time series over the period 2000–2100, calculated using linear regression. As a comparison the vertical component of Eliassen–Palm (EP) flux is included, which gives a measure of wave activity entering the stratosphere (Andrews et al. 1987) as well as the wave-1 and -2 components of geopotential height at 10 hPa. Statistical significance is obtained by calculating the distribution sample error [see Eq. (3)].

Figure 6a shows a consistent decrease in objective area and hence vortex strength throughout the twenty-first century that is significant in most of the winter period. The vortex centroid latitude (Fig. 6b) is consistent with this and shows an equatorward trend in the vortex centroid, at least in early winter. At its maximum, during January, a shift of 0.25° toward the equator is observed per decade. In context this results in a 2.5° equatorward shift in the vortex centroid by the end of the twenty-first century, changing its centroid from 80° to 77.5°N. This would result in a change in the polar-night jet structure and consequently the propagation properties of Rossby waves. Mitchell et al. (2011a) and Hannachi et al. (2011) also showed that the centroid latitude diagnostic was indicative of wave-1 activity, and a change in this diagnostic reflected a change in vortex displacement events. They also showed that changes in the vortex aspect ratio were highly correlated to wave-2 Rossby wave activity, and Fig. 6c shows no great change in this diagnostic. These results indicate that future vortex variability in the simulations is dominated by vortex displacements rather than large-scale vortex-splitting events, a conclusion that is supported by the trends in wave-1 and -2 components of geopotential height, measured at 10 hPa (Figs. 6d,e).

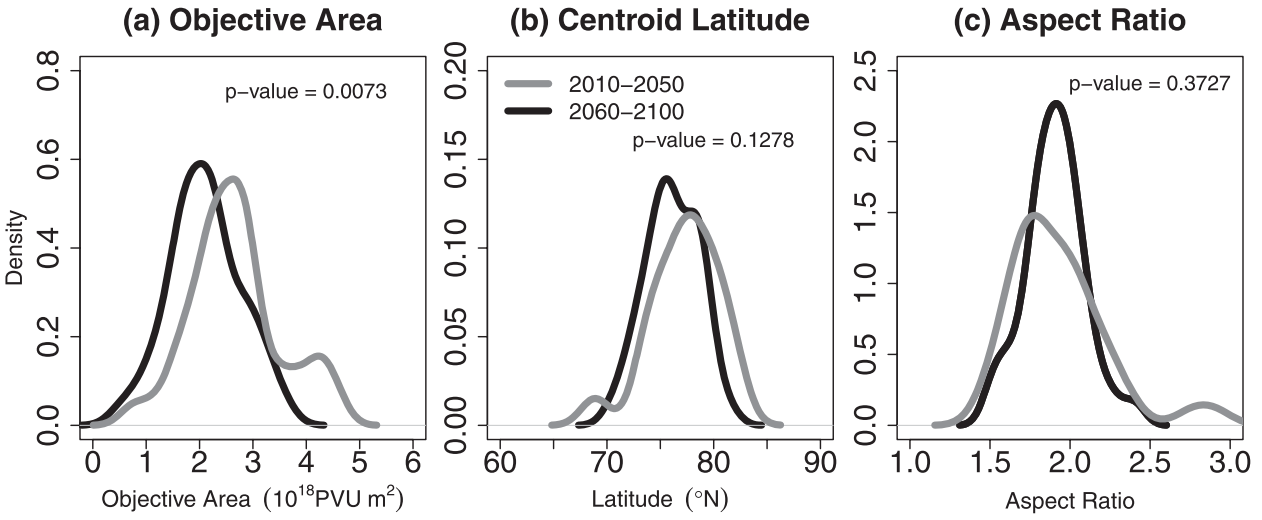

FIG. 7. Probability density plots for the daily mean (a) objective area, (b) centroid latitude, and (c) aspect ratio on the 840-K surface during December between 2010 and 2050 (gray) and 2060 and 2100 (black). The p values are calculated using a Kolmogorov–Smirnov nonparametric significance test.

The EP flux (Fig. 6f) is used as a diagnostics of wave activity and is calculated at 55°N because that is where the largest climatological wave activity is observed, and at 100 hPa to measure waves entering into the stratosphere. Results are sensitive to chosen latitudes outside the extratropics (i.e., outside the 50°–70°N range) but not to the pressure level. Broadly speaking, the EP flux agrees well with the other diagnostics in that December seems to show the largest trend, and this indicates more wave activity entering the stratosphere during this period.

To expand on Fig. 6, the moment diagnostics are examined in terms of their probability density functions (PDFs) for the first half of the twenty-first century (Fig. 7, gray lines), and for the second half (Fig. 7, black lines) for daily data during December (choosing January gave qualitatively similar results) on the 840-K isentropic surface (~10 hPa). These PDFs are calculated from the ensemble mean of the three transient runs, as such shifts in the distributions are far more meaningful than changes in the extremes.

The largest changes in the bulk of data are observed in the distributions of the objective-area (Fig. 7a) and centroid-latitude (Fig. 7b) diagnostics but not in the aspect ratio (Fig. 7c), strengthening the conclusions found from Fig. 6. In particular the objective area shows a shift in its mean state to weaker values, as well as being less variable, and this is significant at the 95% confidence level.[3] The centroid latitude shows a shift in its mean state to a more equatorward position, but with no clear change in its variability. Combining the diagnostics suggests that the vortex becomes consistently weaker and displaced more equatorward toward the end of the twenty-first century.

5. Summary and discussion

Variability of the polar vortex over the twenty-first century has been examined using a state-of-the-art climate model which has both a fully resolved stratosphere and fully coupled ocean, combined with some recently developed vortex-specific diagnostics. We have used three ensemble members of an RCP8.5 simulation to minimize internal model variability, although we note that variability between each ensemble member was large. Summary points from our analysis are as follows:

- There is a significant change in the vortex mean state over the twenty-first century, resulting in a weaker, more disturbed vortex.
- There is no statistically significant change in NH SSW frequency over the twenty-first century when compared with the historical period.
- In the historical period the monthly distribution of SSWs is shifted toward late winter, with most events occurring in February, but as GHG concentrations increase SSWs become more evenly distributed throughout winter.
- An increase in the wave-1 amplitude of between 15 and 20 m decade^{-1} is observed and is consistent with the equatorward shift in the vortex centroid of up to 2.5° in early winter by the end of the twenty-first

[3] Caution must be exercised here as the model did not reproduce the climatology of the objective area well (see Fig. 5).

century, implying more vortex displacement events into the future.

Recent research has suggested that the impact of split- and displaced-vortex events is different both on regional scales and in terms of persistence times (Mitchell et al. 2012a, manuscript submitted to *J. Climate*). An increase in displaced-vortex events over the twenty-first century as predicted here could therefore play an important role in future surface climate projections. For instance, it suggests an increase in surface cold-air outbreaks over Canada, as well as an increase in blocking activity over North America (Mitchell et al. 2012a, manuscript submitted to *J. Climate*).

Additionally, we have shown that although the vortex tends to be in a weaker state toward the end of the twenty-first century, this does not necessarily mean that the frequency of extreme weak vortex events will increase. Indeed, by changing the monthly distribution of SSWs this effect may well happen, although we do note that the very binary nature of the SSW definition is such that the moment-based diagnostics are better for this type of analysis. Finally, we emphasize the importance of using multiple ensemble members in such analyses, especially when using more complex models, as internal model variability can be large.

Acknowledgments. We thank the two anonymous reviews for insightful comments. DMM is supported by a grant from the UK Natural Environmental Research Council (NERC); LJG and SMO are funded by the NERC National Centre for Atmospheric Science (NCAS). The work of SCH and NB was supported by the Joint DECC/Defra Met Office Hadley Centre Climate Programme (GA01101) and the European Commission's 7th Framework Programme COMBINE project 226520. PW is supported by a NERC student grant. We would also like to thank the Stratosphere and Climate groups at the Universities of Reading and Oxford for useful discussions.

REFERENCES

Andrews, D., J. Holton, and C. Leovy, 1987: *Middle Atmosphere Dynamics*. Academic Press, 489 pp.

Baldwin, M., and T. Dunkerton, 2001: Stratospheric harbingers of anomalous weather regimes. *Science,* **294,** 581–584.

——, and D. Thompson, 2009: A critical comparison of stratosphere–troposphere coupling indices. *Quart. J. Roy. Meteor. Soc.,* **135,** 1661–1672.

Bell, C., L. Gray, and J. Kettleborough, 2010: Changes in Northern Hemisphere stratospheric variability under increased CO_2 concentrations. *Quart. J. Roy. Meteor. Soc.,* **136,** 1181–1190.

Butchart, N., and Coauthors, 2011: Multimodel climate and variability of the stratosphere. *J. Geophys. Res.,* **116,** D05102, doi:10.1029/2010JD014995.

Charlton, A., and L. Polvani, 2007: A new look at stratospheric sudden warmings. Part I: Climatology and modeling benchmarks. *J. Climate,* **20,** 449–469.

——, A. O'Neill, W. Lahoz, A. Massacand, and P. Berrisford, 2005: The impact of the stratosphere on the troposphere during the Southern Hemisphere stratospheric sudden warming, September 2002. *Quart. J. Roy. Meteor. Soc.,* **131,** 2171–2188.

——, and Coauthors, 2007: A new look at stratospheric sudden warmings. Part II: Evaluation of numerical model simulations. *J. Climate,* **20,** 470–488.

Charlton-Perez, A., L. Polvani, J. Austin, and F. Li, 2008: The frequency and dynamics of stratospheric sudden warmings in the 21st century. *J. Geophys. Res.,* **113,** D16116, doi:10.1029/2007JD009571.

Charney, J., P. Drazin, and Coauthors, 1961: Propagation of planetary-scale disturbances from the lower into the upper atmosphere. *J. Geophys. Res.,* **66,** 83–109.

Clough, S., and M. Iacono, 1995: Line-by-line calculation of atmospheric fluxes and cooling rates. 2. Application to carbon dioxide, ozone, methane, nitrous oxide and the halocarbons. *J. Geophys. Res.,* **100,** 16 519–16 535.

Esler, J., L. Polvani, and R. Scott, 2006: The Antarctic stratospheric sudden warming of 2002: A self-tuned resonance? *Geophys. Res. Lett.,* **33,** L12804, doi:10.1029/2006GL026034.

Fels, S., J. Mahlman, M. Schwarzkopf, and R. Sinclair, 1980: Stratospheric sensitivity to perturbations in ozone and carbon dioxide: Radiative and dynamical response. *J. Atmos. Sci.,* **37,** 2265–2297.

Hannachi, A., D. Mitchell, L. Gray, and A. Charlton-Perez, 2011: On the use of geometric moments to examine the continuum of sudden stratospheric warmings. *J. Atmos. Sci.,* **68,** 657–674.

Hardiman, S., N. Butchart, T. Hinton, S. Osprey, and L. Gray, 2012: The effect of a well-resolved stratosphere on surface climate: Differences between CMIP5 simulations with high and low top versions of the Met Office climate model. *J. Climate,* in press.

Jones, C., and Coauthors, 2011: The HadGEM2-ES implementation of CMIP5 centennial simulations. *Geosci. Model Dev. Discuss.,* **4,** 689–763.

Martin, G., and Coauthors, 2011: The HadGEM2 family of Met Office Unified Model Climate configurations. *Geosci. Model Dev. Discuss.,* **4,** 765–841.

Matthewman, N., J. Esler, A. Charlton-Perez, and L. Polvani, 2009: A new look at stratospheric sudden warmings. Part III: Polar vortex evolution and vertical structure. *J. Climate,* **22,** 1566–1585.

McLandress, C., and T. Shepherd, 2009: Impact of climate change on stratospheric sudden warmings as simulated by the Canadian Middle Atmosphere Model. *J. Climate,* **22,** 5449–5463.

Mitchell, D., A. Charlton-Perez, and L. Gray, 2011a: Characterizing the variability and extremes of the stratospheric polar vortices using 2D moment analysis. *J. Atmos. Sci.,* **68,** 1194–1213.

——, L. Gray, and A. Charlton-Perez, 2011b: The structure and evolution of the stratospheric vortex in response to natural forcings. *J. Geophys. Res.,* **116,** D15110, doi:10.1029/2011JD015788.

——, and Coauthors, 2012b: The nature of arctic polar vortices in chemistry–climate models. *Quart. J. Roy. Meteor. Soc.,* in press.

Rind, D., D. Shindell, P. Lonergan, and N. Balachandran, 1998: Climate change and the middle atmosphere. Part III: The doubled CO_2 climate revisited. *J. Climate,* **11,** 876–894.

Schoeberl, M., and D. Hartmann, 1991: The dynamics of the stratospheric polar vortex and its relation to springtime ozone depletions. *Science,* **251,** 46–52.

Son, S.-W., and Coauthors, 2008: The impact of stratospheric ozone recovery on the Southern Hemisphere westerly jet. *Science,* **320,** 1486–1489.

——, and Coauthors, 2010: Impact of stratospheric ozone on Southern Hemisphere circulation change: A multimodel assessment. *J. Geophys. Res.,* **115,** D00M07, doi:10.1029/2010JD014271.

Thompson, D., M. Baldwin, and J. Wallace, 2002: Stratospheric connection to Northern Hemisphere wintertime weather: Implications for prediction. *J. Climate,* **15,** 1421–1428.

Waugh, D., 1997: Elliptical diagnostics of stratospheric polar vortices. *Quart. J. Roy. Meteor. Soc.,* **123,** 1725–1748.

——, and W. Randel, 1999: Climatology of Arctic and Antarctic polar vortices using elliptical diagnostics. *J. Atmos. Sci.,* **56,** 1594–1613.

——, L. Oman, S. Kawa, R. Stolarski, S. Pawson, A. Douglass, P. Newman, and J. Nielsen, 2009: Impacts of climate change on stratospheric ozone recovery. *Geophys. Res. Lett.,* **36,** L03805, doi:10.1029/2008GL036223.

Woollings, T., A. Charlton-Perez, S. Ineson, A. Marshall, and G. Masato, 2010: Associations between stratospheric variability and tropospheric blocking. *J. Geophys. Res.,* **115,** D06108, doi:10.1029/2009JD012742.

CORRIGENDUM

DANIEL M. MITCHELL, SCOTT M. OSPREY, AND LESLEY J. GRAY

National Centre for Atmospheric Science, University of Oxford, Oxford, United Kingdom

NEAL BUTCHART AND STEVEN C. HARDIMAN

Met Office Hadley Centre, Exeter, United Kingdom

ANDREW J. CHARLTON-PEREZ

Department of Meteorology, Reading University, Reading, United Kingdom

PETER WATSON

Atmospheric, Oceanic, and Planetary Physics, University of Oxford, Oxford, United Kingdom

(Manuscript received and in final form 13 August 2012)

There was a numerical error in the abstract of Mitchell et al. (2012). In the fourth sentence of the abstract the number should be 7 events per decade, not 0.7. The full sentence should read, ''Analysis of the standard stratospheric zonal mean wind diagnostic shows no significant increase over the twenty-first century in the number of major sudden stratospheric warmings (SSWs) from its historical value of 7 events per decade, although the monthly distribution of SSWs does vary, with events becoming more evenly dispersed through the winter.''

The staff of the *Journal of the Atmospheric Sciences* regrets any inconvenience this error may have caused.

REFERENCE

Mitchell, D. M., S. M. Osprey, L. J. Gray, N. Butchart, S. C. Hardiman, A. J. Charlton-Perez, and P. Watson, 2012: The effect of climate changes on the variability of the Northern Hemisphere stratospheric polar vortex. *J. Atmos. Sci.,* **69,** 2608–2618.

Corresponding author address: Daniel Mitchell, Atmospheric, Oceanic, and Planetary Physics, University of Oxford, Oxford OX1 3PU, United Kingdom.
E-mail: mitchell@atm.ox.ac.uk

DOI: 10.1175/JAS-D-12-0234.1